

Influence of Chip Serration Frequency on Chatter Formation During End Milling of Ti6Al4V

Md. Anayet U. Patwari

Department of Mechanical and Chemical Engineering,
Islamic University of Technology,
Gazipur Dhaka 1704, Bangladesh

A. K. M. Nurul Amin¹

Department of Manufacturing and Materials Engineering,
International Islamic University of Malaysia,
53100 Kuala Lumpur, Malaysia
e-mail: akamin@iiu.edu.my

Waleed F. Faris

Department of Mechanical Engineering,
Faculty of Engineering,
International Islamic University of Malaysia,
53100 Kuala Lumpur, Malaysia

This paper includes the findings of an experimental study on instabilities of the chip formation process during end milling of Ti6Al4V alloy and the influence of these instabilities on chatter formation. It has been identified that the chip formation process has a discrete nature, associated with the periodic shearing process during machining. The chip formed during machining of titanium alloy Ti6Al4V is found to be mainly with primary serrated teeth appearing in the main body of the chip. Secondary serrated teeth resulting from the coagulation of a certain number of primary serrated teeth also happen to appear at the free or constrained edge of the chip, especially when the system enters into chatter. In order to identify the interaction of these chip instabilities with the prominent natural vibration of the machine tools system components, the different mode frequencies of the vibrating components of the system have been identified using experimental and finite element modal analyses, and vibration responses during actual cutting have also been recorded using an online vibration monitoring system. The vibration signals in frequency domain (fast Fourier transform) have been analyzed to identify the chatter frequencies and the peak amplitude values. Chatter was found to occur at two dominant mode frequencies of the spindle. These mode frequencies at which chatter occurred have been compared with the chip serration frequencies in a wide cutting speed range for different conditions of cutting. It has been concluded from these findings that chatter occurs during end milling due to the resonance of the machine tools system component when the frequency of primary serrated teeth formation is approximately equal to the "prominent natural frequency" modes of the system components, which are the two mode frequencies of the VMC machine spindle in this particular case.

[DOI: 10.1115/1.4003478]

Keywords: discreteness of chip formation, chip serration frequency, prominent natural frequencies, resonance and chatter

1 Introduction

High metal removal rate with a desired quality of surface finish, which is the ultimate objective in machining, depends on a large number of factors, which include chip-tool interaction, cutting temperature, wear mechanism and wear rate, cutting force, chatter, and dynamics behavior of the machine tools system. Appearance of chatter during metal cutting leads to instability of the system, which adversely affects surface quality of the machined parts, lowers tool life, and generates irritating noise. Although chatter has been extensively investigated in the past 40 years, it is still very difficult to suppress it in practice. Hypotheses developed over the years are mainly as mentioned below. Taylor suggested that element chip formation is responsible for chatter [1], but this proposition was not acceptable since element chip formation occurs at extremely low cutting speed where chatter is almost absent. However, discreteness in metal cutting at higher speeds may cause chatter. Kudinov [2] and Shteinberg [3] postulated that the periodic effect of built-up-edge (BUE) formation is responsible for chatter. Kuznetsov [4] also considered that the vibration caused by the unstable and periodically broken BUE is responsible for chatter. However, no serious chatter is also observed in the cutting speed range of BUE formation; chatter generally exists at relatively higher cutting speeds where BUE is absent. Eliasberg

[5] considered that the cause of chatter is the formation of a crack in the chip above the tool point, which is observed when the cutting process is monitored using a high speed cine camera. However, Loladze [6] established that at higher cutting speeds, the chip fully adheres to the tool surface and as such, there cannot be any crack formed in the chip ahead of the tool point at those cutting speed ranges, so it cannot be accepted as the physical cause of chatter. Doi [7], Doi and Kato [8], and later Kato [9] concluded based on their experiments on orthogonal cutting on a reasonably flexible work-piece that chatter was established primarily due to a phase lag of the cutting force with respect to the fluctuation of chip thickness. It was found that force fluctuations lag the vibration movement. It was postulated that due to this lag effect, some energy is left available in each oscillation to maintain the vibration. These ideas were also supported by the work of Tashlickii [10]. However, Smith [11] and later Smith and Tobias [12] suggested that the findings of Doi and Kato on the force phase lag were primarily because of the low frequency of vibration. It was found that as the frequency was increased, the phase difference decreased and at even higher frequencies, the force fluctuations preceded the vibration movement. Tobias [13] first mentioned about the chip-thickness variation effect (regenerative effect). He mentioned that this effect occurs with single-edged tools, such as lathe tools, when the cutting edge of the tool traverses a wavy surface on the work generated by the previous cut. However, the experimental works conducted by Eliasberg [5] and Amin [14], and Patwari [15] contradicted the regenerative chatter theory. They found that during turning under certain cutting conditions and system parameters, there are ranges of cutting speed where chatter occurred at nearly constant frequencies. In

¹Corresponding author.

Contributed by the Manufacturing Engineering Division of ASME for publication in the JOURNAL OF MANUFACTURING SCIENCE AND ENGINEERING. Manuscript received May 22, 2010; final manuscript received January 7, 2011; published online February 16, 2011. Assoc. Editor: Suhas Joshi.

these speed ranges, vibration marks left from previous cut did not have any influence on the resultant chatter frequency since at higher cutting speed the frequency rains constant and hence the pitch of the chatter marks increases and the tool does not follow the pattern on the cutting surface from the previous cut. If chatter is to appear in the system, the pitches of the waviness of the previous and the current cut were required to be equal and they ought to have been in opposite phases as postulated by the “regenerative chatter theory,” which is not the case here. One can then argue what leads to chatter under these conditions if regenerative force is not its cause. Amin [14] and Patwari [16,17] found that the root cause of chatter lies in the coincidence of the frequency of *instability of chip formation* with any one of the natural frequencies of the machine tool system components. The instability of chip was found to be due to the formation of *cyclic chip*, widely known as the *serrated* or *saw toothed chips*. The mechanism of this cyclic chip formation was well documented by Armarego [18]. El Mansori [19] in his works observed that with the controlling of chip serration by magnetically assisted controlled cutting process, the tool life significantly increased, which gives a close indication about the beating effect of chip serration frequency on tool surface. Amin [20] in his experimental investigations on the turning process found that when the frequency of formation of the primary or secondary serrated teeth of the chip coincided with any one of the natural frequencies of the system, resonance occurred resulting in high vibration amplitudes of the respective system components. These vibrations with high amplitudes are well known as resonance in metal cutting. Amin’s works were focused on turning operation and hence there is a need for further studies to understand the physical causes of chatter during milling operation to be able to explain the behavior of the machine tool system when it is in a state of chatter so that the issue of chatter control for milling can be addressed more effectively.

1.1 Aims and Objectives of the Present Work. The main objectives of the present were the following:

1. to identify the mode frequencies of the different components of the machine tool system by experimental method and to verify the same using finite element (FE) modal analysis
2. to study the morphology of chip formed during end milling of Ti6Al4V to investigate the presence of primary and secondary serrated teeth and to determine the frequencies of their formative cycles
3. to study the frequency-amplitude characteristics of vibration/chatter under variable cutting and system parameters to determine the role of the frequency of chip serration and the mode frequencies of prominent machine tool system components in chatter formation
4. to identify the mechanism of chatter formation in end milling of Ti6Al4V

2 Experimental Setup

The main thrust of the experiments was on the study of chips and monitoring of vibrations during end milling of titanium alloy-Ti6Al4V. For studying the chips, scanning electron microscope (SEM) and optical microscope were used. For monitoring the vibration, an especially designed vibration monitoring system comprising accelerometer, a 16 channel rack and a high speed DAQ card were used. Datalog DASY Lab 5.6 was used for signal analysis and processing. The main software modules used are the amplitude-time display (time domain), the fast Fourier transform (FFT) display (frequency domain). Frequency range of interest was 0–12,500 Hz. FFT was used for changing the signals from the time to the frequency domain using the power density spectrum.

Cutting tests were conducted mainly on Vertical Machining Center (VMC ZPS, model 1060) powered by a 30 kW motor with a maximum spindle speed of 8000 rpm. Figure 1 shows the experimental setup for the cutting tests conducted on end milling of Ti6Al4V.

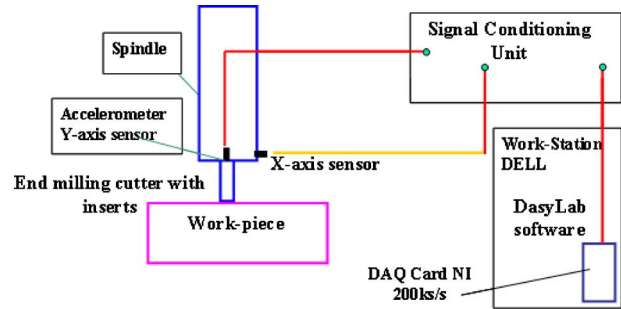


Fig. 1 Experimental setup for end milling

2.1 Tool (Inserts). SANDVIK grade PM1030 carbide inserts of code: R390-11 T3 08E-PL were used in the cutting tests. Insert coating material was TiN. Insert geometry is shown in Fig. 2.

2.2 Experimental Conditions. Cutting speeds were varied in the range of 20–100 at an interval of 10 min/min and verification was done at the middle of the interval where necessary (35 m/min) and axial depth of cut were 2.0 mm and 2.2 mm and feed value were 0.089 mm/tooth, 0.16 mm/tooth, and 0.204 mm/tooth.

2.3 Experimental Procedures

2.3.1 Modal Analysis-Mode Shape Frequencies. Free vibration analysis of the relevant components of the vertical machining center was conducted [21] using the following procedure: Forced excitation was given to the system using a plastic hammer/mallet. The free vibration data were sensed in the frequency domain by an accelerometer attached to the element opposite to the point of impact. Figure 3 shows the experimental modal analysis power spectrum responses (FFT) for Collet and Spindle casing of vertical machining center.

2.3.2 Operational Modal Analysis. Operational modal analysis is based on measuring only the output of a structure and using the ambient and operating forces as unmeasured input. It is used instead of classical mobility-based modal analysis for accurate modal identification under actual operating conditions and in situations where it is difficult or impossible to control an artificial excitation of the structure.

In the milling machine structure, the inner spindle is surrounded by the outer spindle; as a result, it is not possible to extract the mode shape using knocking test. Operational modal analysis was carried out to find out the mode shape of the inner spindle under load and no load conditions, as shown in Fig. 4.

2.3.3 FE Analysis. In order to generate a finite element model of the machine tool, a three-dimensional geometrical model of machine’s structure was developed using CATIA software and then converted to. igs format for further analysis by ABAQUS software. The finite element analysis (FEA) model provides natural values and response frequency extraction capabilities. The natural vibra-

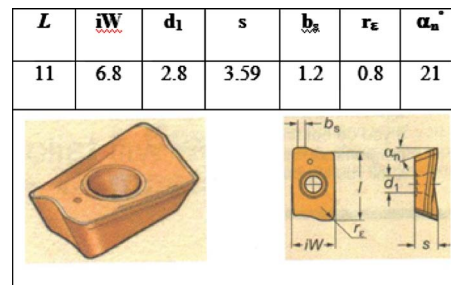


Fig. 2 Insert shape and geometry

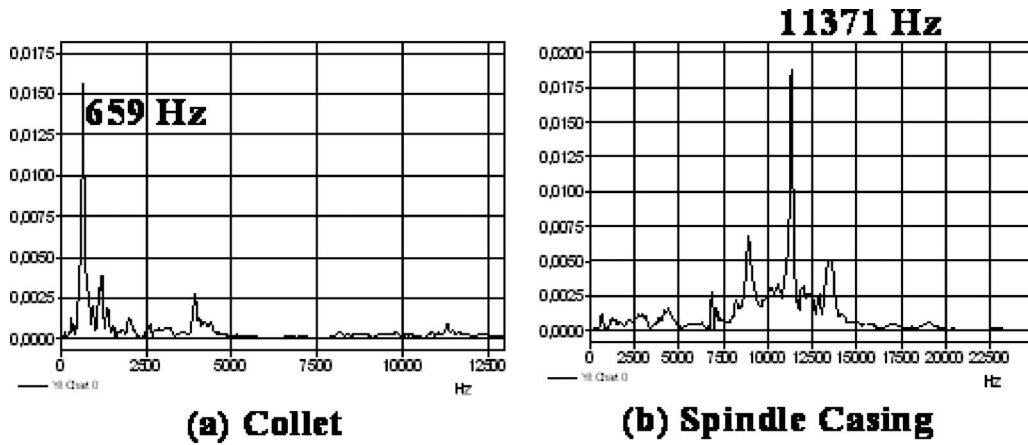
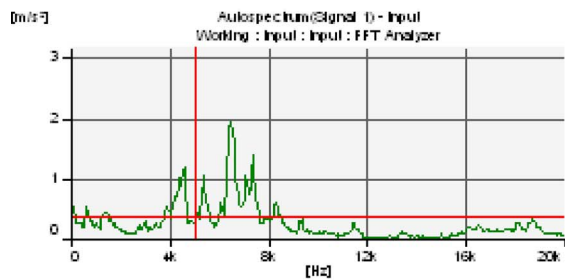


Fig. 3 Experimental modal analysis power spectrum responses (FFT) for (a) Collet and (b) spindle casing of vertical machining center

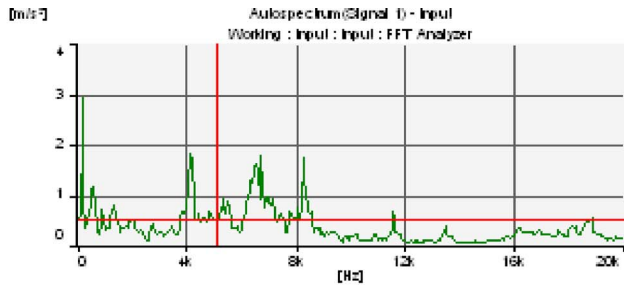
tion modes of the machine tool components are three-dimensional shapes that provide better capability to analyze their vibration modes. The model was applied to the given vertical machining center. After model selection, the necessary input data on material properties, such as modulus of elasticity, Poisson ratio, and density were applied. Quadratic tetrahedral elements were used in the finite element method (FEM) model for mesh generation. The element distribution was uniform and the element dimensions were finer and more controlled for the parts with relatively small dimensions like spindle, tool holder, and collect. Afterwards,

boundary conditions on different components were applied and finally modal analysis was performed to obtain natural frequencies of the system components. In continuation, fine screening of the finite element model was accomplished to investigate the matching of the natural frequencies obtained for FE analysis and those from the experimental modal analysis. A sample of the eigenmodes of the different components of the vertical machining center components are shown in Fig. 5.

The different dominating mode shapes of the components of the vertical machining center extracted from the experimental and FE

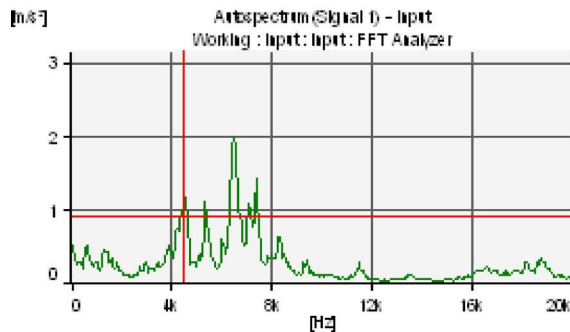


1000 RPM

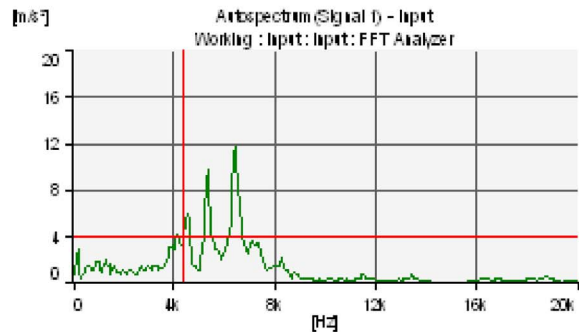


3500 RPM

Spindle mode shape: 4394 Hz, 6866 Hz, 8294 Hz



1000 RPM



3500 RPM

Spindle mode shape: 4394 Hz, 6866 Hz, 8294 Hz

Fig. 4 Operational Modal analysis of inner spindle: (a) under no load and (b) load conditions

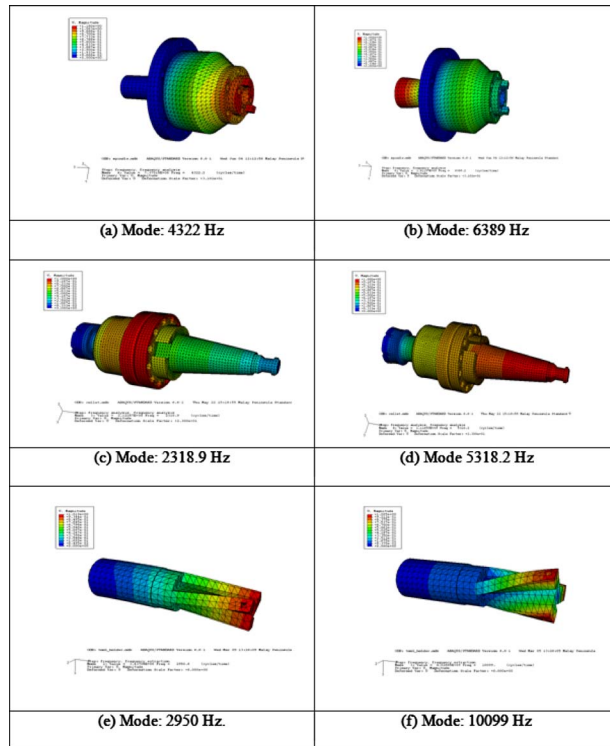


Fig. 5 Selected eigenmodes of the different machine components of vertical machining center

modal analyses are listed in Table 1.

It can be observed from Table 1 that the different natural mode frequencies of the different components of the vertical machining center predicted by FE analysis and determined by experimental modal analysis shows good agreement (within a range of $\pm 10\%$ deviation), except for a limited number of cases. The variations of the theoretical frequencies from the experimental values in the case of the tool holder are 41.5%, 13.5%, and -7.9% for frequencies 2081 Hz, 8892 Hz, 11352 Hz, respectively. The variations being -1.6% , -6.9% , and -3.5% for frequencies 4394 Hz, 6866 Hz, and 8294 Hz, respectively, of the inner spindle, 5.7% and -9.5% for frequencies 9009 Hz and 11,371 Hz, respectively, of the outer spindle and finally 17%, 14.1%, -7.1% , and 2.9% for frequencies 659 Hz, 2032 Hz, 3955 Hz, and 5169.7 Hz, respectively, of the Collet.

2.3.4 Primary and Secondary Serrated Teeth and Calculation of Chip Serration Frequency. A method for calculating the frequency of instability of chip formation has been developed and the formula for calculating the frequency of instability of chip formation has been derived. The method employed for chip analysis is simple and efficient, especially in cases where a great number of samples must be examined. Considerable amount of time for chip mounting and preparation is alleviated. The chips are first

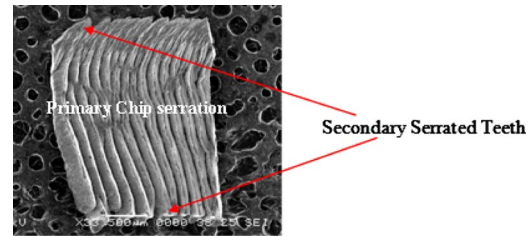


Fig. 6 SEM top view of the chip with the serrated elements (cutting speed of 40 m/min, depth of cut 2.2 mm, and feed 0.16 mm/tooth) during machining of Ti6Al4V

broken and untwirled to make them straight and suitable for observation. The segments are then observed under scanning electron microscope (SEM) to have a close look at the chip to identify its morphology and to inspect the presence of the primary and/or the secondary serrated teeth and any other type of instability that might be present in the outer view of the chip. A sample of SEM view of the chip is shown in Fig. 6, which indicates the presence of the mainly the primary serrated teeth during machining the given titanium alloy (Ti6Al4V). It is to be noted here that chips formed during machining of titanium and its alloys exhibit mainly this type of distinct serrated teeth, which are formed due to the adiabatic shear process [22]. These teeth appear at the main cross section of the chip (Fig. 6).

Since it was observed in the present work that the primary serrated teeth played more prominent role in chatter formation during machining of Ti6Al4V, the attention was paid on calculating their frequency of formation. The number of primary serrated teeth was counted within the length of the chip in the SEM picture along the middle section of the chip to avoid the secondary serrated teeth. The frequency of primary serration, F_c , was then calculated knowing the length of the chip in the SEM pictures, L , the coefficient of (b) linkage, K (determined by dividing the uncut chip length by the actual chip length), cutting speed, V m/min, and the number of secondary serrated teeth, n , observed on the SEM picture within the same length of the chip. The following formula was used for the calculation:

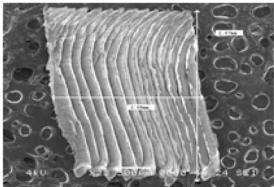
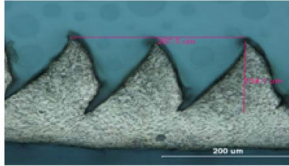
$$F_c = 1000 \frac{nV}{60(LK)} [\text{Hz}] \quad (1)$$

The counting was conducted on different chip samples at a given speed to avoid random errors and to ensure repeatability of the experimental results. Apart from that experimental results at ten different cutting speeds have been included in this paper, the calculated frequencies are found to be consistently increasing with the cutting speed. The authors of the present work also came up with models for identifying and predicting the chip serration frequency for various work materials using statistical tools and thus the repeatability of the experimental results on chip serration frequency has been also verified in previous works [23,24].

Table 1 Dominating mode shapes of different components of vertical machining center

| System component | Tool holder | Inner spindle | Outer spindle | Collet |
|-----------------------------|--------------------|------------------|---------------|-------------------------|
| Experimental modal analysis | | | | |
| Dominating mode shape (Hz) | 2081, 8892, 11352 | 4394, 6866, 8294 | 9009, 11371 | 659, 2032, 3955, 5169.7 |
| Theoretical FE analysis | | | | |
| Dominating mode shape (Hz) | 2944, 10099, 10454 | 4322, 6389, 8004 | 9520, 10291 | 771, 2319, 3674, 5318 |

Table 2 Determination of chip serration frequency

| | | | |
|--|--|---|--|
|  <p>(a) SEM View, DOC:2.2</p> | |  <p>(b) Length wise sectional View</p> | |
| SEM and optical microscope views of the chip at with depth of cut 2.2 mm and feed 0.16 mm/tooth shown in (a) and (b) respectively. | | | |
| Measuring parameters | | | |
| Cutting Speed: 60m/min No of Serrated Teeth (average): 16 Length in SEM: 2.08 mm Uncut chip length: 31.44mm Actual length: 30.5 mm Chip shrinkage coefficient: 1.03 | | Cutting Speed: 60m/min No of Serrated Teeth: 2 Length in Microscope: 0.26mm Uncut chip length: 31.44mm Actual length: 30.5 mm Chip shrinkage coefficient: 1.03 | |
| Determination of chip serration frequency | | | |
| Calculated serrated frequency: $f_c = \frac{1000 \times 60 \times 16}{60(2.08 \times 1.03)} = 7468 \text{ Hz}$ | | Calculated serrated frequency: $f_c = \frac{1000 \times 60 \times 2}{60(0.26 \times 1.03)} = 7468 \text{ Hz}$ | |

2.3.5 *Example of Determination of Chip Serration Frequency.* The sample of the calculation procedure for the chip serration frequency is shown in Table 2 for both the SEM and optical microscope views of the chip at same cutting condition. It has been observed that the chip serration frequencies calculated for both the cases are the same.

3 Results and Discussion

3.1 Analysis of Chips Produced in End Milling. Two types of investigations were conducted on the chips formed during the end milling tests. First, the chips were observed under the SEM and second ground, polished and etched lengthwise microsections of chips at various cutting conditions were viewing under the optical microscope to capture the structure of the chip and also count the number of primary serrated elements within a given length of the chips. SEM top views and the microsections of chips at some selected cutting speeds are shown side by side in Fig. 6. From this figure, it observed that the Ti6Al4V chips have characteristic primary serrated teeth formed as a result of the adiabatic shear process [22]. The mechanism of formation of the primary serrated teeth was also studied by Talantov et al. [25], Amin [14], and other researchers. The primary serrated teeth were termed as “cyclic chips” in the works of Amin and Talantov et al., since they follow a given formative cycle, which consists of two phases, the phase of compression and the phase of shear. During the phase of compression, the shear plane rotates in the direction of reduction of the shear angle. During this phase, fresh incoming chips accumulated on the rake face of the tool with very little deformation of the chip grains. During this phase, shear stresses gradually build up along the shear zone and the next phase starts when the shear stresses reach the yield strength of the material. Shearing takes place along a narrow rotating shear zone. Shear plane angle increases during this phase in accordance with the minimum energy

principle of metal cutting. Shearing is an adiabatic process since the heat conductivity of the material is either too low, as in the cases of titanium alloys, or the time for dissipation of the heat generated during the instant shear process is too low when cutting is performed at high cutting speeds for carbon and alloy steels.

At some specific cutting conditions, secondary serrated teeth are also formed, at either the free or the constrained edge of the chip, combining a certain number of primary serrated teeth. It can be also observed from Fig. 6 that “secondary serrated teeth” are formed as a combination of two or more primary teeth at one of the edges of the chip, while there are also teeth with close pacing at the other edge (Fig. 6). These teeth have been termed in this paper as “secondary serrated” teeth to distinguish them from the primary serrated teeth. Though these teeth are sometimes the reflections of different chatter harmonics or natural vibrations of the system, Amin [14] and Amin et al. [26,27] observed that during machining of ductile materials like carbon steel and stainless steel regularly spaced “secondary” serrated teeth start appearing from very low speed and the frequency of their formation increases with cutting speed. These teeth are found to be responsible for chatter formation during turning and end milling of ductile materials. SEM top view of chip produced during machining of carbon steel AISI 1040 indicating the presence of such “secondary serrated” teeth is shown in Fig. 7 [26].

Different parameters of the chip (coefficient of chip shrinkage, chip lengths, L, in the SEM views, number of serrated elements within length L, for different speed, feed and depth of cut values, and the corresponding chip serration frequency values, calculated using Eq. (1)) are shown in Table 3. The calculated values of the primary chip serration frequency are also indicated for different cutting speeds, in the Fig. 8.

General observation from Fig. 8 shows that chips have mainly the primary saw teeth, which are produced due to the alternative phase compression and adiabatic shear process [22] resulting in fluctuation of the cutting force exerted on the tool. The primary

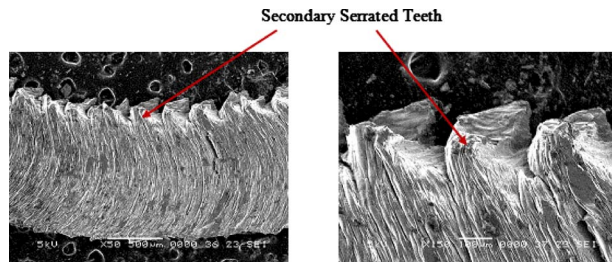


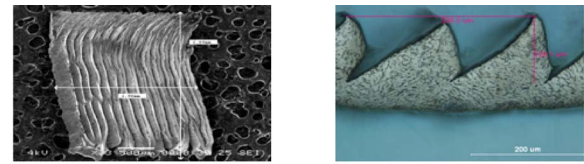
Fig. 7 Chip formed by cutting the carbon steel AISI 1045 at 2 mm depth of cut, 200 m/min with overhang of 60 mm with (a) 50× and (b) 150× magnifications [26]

serrated teeth are formed at the main body of the chip at almost equal pacing. Primary serrated teeth formation is the outcome of the inherent discrete behavior of the chip formation process. Cross sectional views of the chips, as shown in Fig. 8(b), reveal that the primary serrated elements undergo alternate phases of compression and shear for the formation of saw teeth. Effort has been also made in Sec. 3.2 to link the frequencies of chip primary serrated teeth with vibration/chatter frequencies.

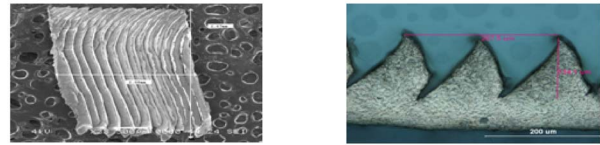
3.2 Analysis of Vibration During Actual Machining. For recording the vibration data, a single sensor was mounted at the stationary outer spindle casing. FFT output in power spectrum for Ti6Al4V alloy were analyzed and the highest vibration peaks and the corresponding excited frequencies at every cutting condition were recorded. Typical FFT outputs in power spectrum at various cutting speed both during cutting and no cutting conditions are shown in Fig. 9. In the investigated cutting speed range, the most significant vibrations that are recorded correspond to the two major mode shape (close to 4394 Hz and 6866 Hz) of the inner spindle and (8892 Hz and 11352 Hz) of the tool holder, as observed from the figure.

3.3 Relationship Between Chip Serration Frequency and Vibration/Chatter Frequency in End Milling at Different Cutting Speeds. The relevant modes (natural frequencies) of the spindle and the changes in primary serration frequencies (from Table 3) with cutting speed are plotted in Fig. 10. Peak acceleration amplitudes for the two natural frequencies of the spindle (from Fig. 9) are plotted against cutting speed in Fig. 11 and against peak frequency to natural frequency ratios, w/w_n , in Fig. 12. After careful comparison of Figs. 9–12, the following observations are made.

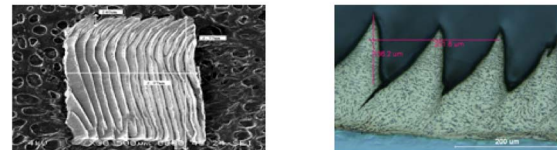
Primary serration frequency increases with cutting speed but when it approaches the range of the inner spindle's first mode shape (first natural frequency) (4394 Hz), the former tends to be almost constant over a range of cutting speed (30–35 m/min) and



Cutting Speed: 35 m/min; Calculated primary chip serration frequency : 4,135 Hz



Cutting Speed: 60 m/min; Calculated Primary chip serration: 7,468 Hz



Cutting Speed: 100 m/min; Calculated Primary chip serration: 13,506 Hz

Fig. 8 Chip morphology: (a) SEM view and (b) lengthwise sectional view (under optical microscope) and the frequencies of the primary serrated teeth at different cutting speeds with feed and depth of cut maintained constant at 0.16 mm/tooth and 2.2 mm, respectively

only after crossing that range it continues to increase again (Fig. 10). A similar behavior is also observed when the chip serration frequency approaches the second mode shape (second natural frequency) of the spindle (6866 Hz); it tends to be almost constant again over a range of cutting speed (55–65 m/min), as shown in Fig. 10. Similar observations were also made by Amin [14] during turning. In the FFT diagram of cutting speed 35 m/min, as shown in Fig. 9(c), it has been observed that the primary chip serration frequency is almost close to the mode shape (4394 Hz) of inner spindle the result is chatter formation (vibration with high acceleration amplitude of the system components) due to resonance. When the chip serration frequency exceeds the range of the mode shape, the next dominating mode shape of the weak components gets excited again due to the resonance and leads the formation of chatter again as shown in Figs. 9(d) and 9(e) and Fig. 10.

It can be observed from Fig. 11 that no severe vibrations are observed in any one of the spindle's two modes (natural frequencies) below the cutting speed of 20 m/min where the chip frequency is below these two spindle modes (natural frequencies), but amplitude starts to increase from the speed of 30 m/min and

Table 3 Parameters of the chips and the chip serration frequencies at different cutting conditions

| Cutting speed (m/min) | No. of serrated teeth | Chip shrinkage coefficient ^a | Chip length in SEM (mm) | Frequency of chip serration (Hz) |
|-----------------------|-----------------------|---|-------------------------|----------------------------------|
| 20 | 23 | 1.16355 | 2.14 | 3,078 |
| 30 | 18 | 1.01342 | 2.23 | 3,982 |
| 35 | 15 | 1.07959 | 1.96 | 4,135 |
| 40 | 17 | 1.08331 | 1.924 | 5,437 |
| 50 | 11 | 1.083 | 1.45 | 5,836 |
| 60 | 16 | 1.03 | 2.08 | 7,468 |
| 70 | 15 | 1.0051 | 1.9 | 9,205 |
| 80 | 15 | 1.01342 | 1.85 | 10,668 |
| 100 | 17 | 1.01 | 2.07 | 13,506 |

^aThe variation in chip shrinkage coefficient was within ±5%.

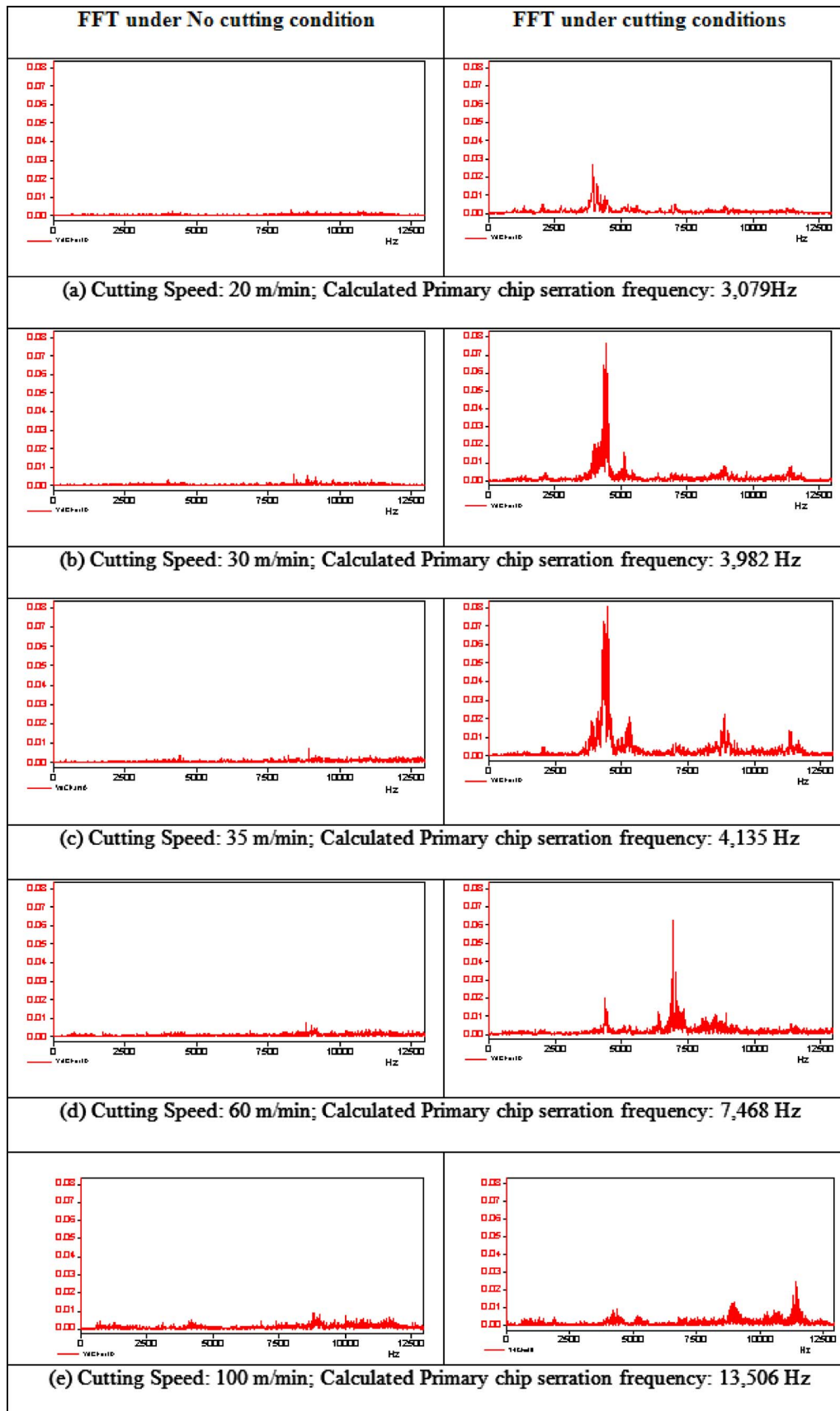


Fig. 9 FFT power spectra of vibrations during machining for end milling at different cutting speeds with feed 0.16 mm/tooth and depth of cut 2.2 mm

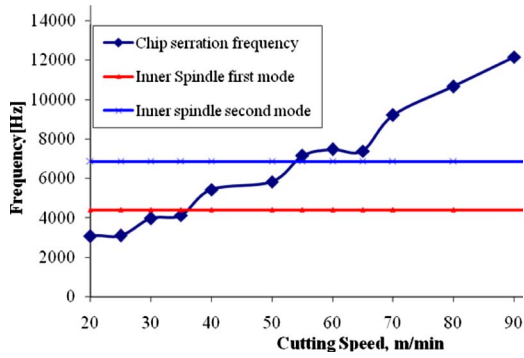


Fig. 10 Mechanism of chip serration in end milling

attains the maximum value at the speed of 35 m/min. At the speed of 35 m/min, the acceleration amplitude peak assumes the highest value when the chip serration frequency value (4135 Hz) is approximately equal to the natural frequency of the inner spindle's first mode shape (4394 Hz). The second mode shape (natural frequency) (6866 Hz) of the inner spindle starts getting excited when the chip serration frequency comes close to this range. It has been observed that at the speed of 60 m/min, acceleration amplitude reaches the maximum values when the chip serration frequency (7247 Hz) is approximately equal to the natural frequency of the inner spindle second mode shape (6866 Hz) (Fig. 11).

It has been further observed from Fig. 12 that when the ratio of the chip serration frequency and the natural frequency of the "main weak" component; i.e., the spindle is close to one there is a peak with maximum acceleration amplitude. This is true for both the mode shapes (natural frequencies) of the spindle.

3.4 Effect of Different Depths of Cut on Serrated Teeth Formation Frequency and Its Relation to Chatter Frequency. The chips formed during end milling of Ti6Al4V at four different depths of cut are investigated. Typical SEM pictures of chips formed under different depth of cut for the same cutting speed and

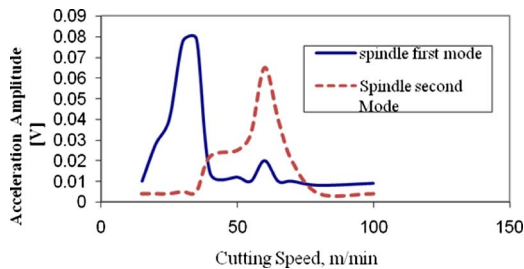


Fig. 11 Effect of cutting speed on acceleration amplitude at different mode shapes

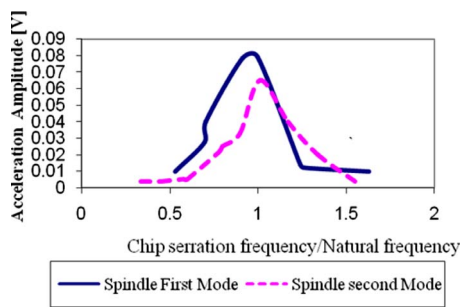


Fig. 12 Variation of acceleration amplitude against ratio of w and w_n for the two mode shapes (natural frequencies) of the spindle

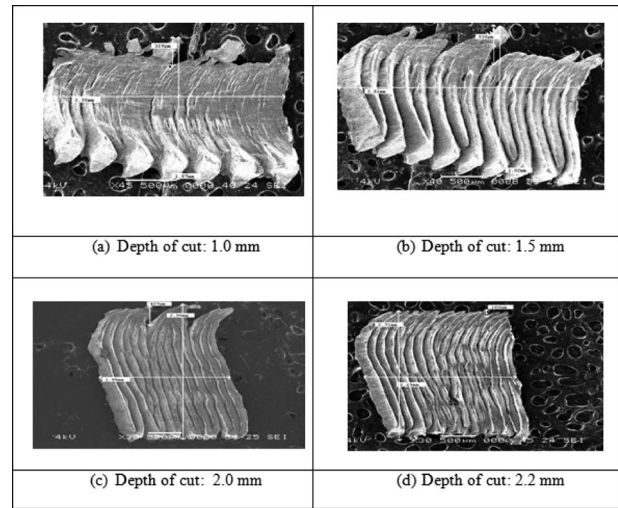


Fig. 13 SEM views of chip for different depths of cut (2.0 mm and 2.2 mm) at cutting speed of 30 m/min and feed value of 0.16 mm/tooth with full immersion

feed are shown in Fig. 13. It has been also found that at all these depths of cut values, the chip formation presents extreme cases of primary and in some cases secondary chip serration. The primary serrated teeth are observed at the main body of the chip at almost equal spacing, whereas the secondary serrated elements are found to be formed at certain conditions as a result of combination of a few primary serrated teeth at the free and/or the constrained edges of the chip (Figs. 12(a)–12(c)). The serration frequency for the primary teeth is calculated at different depths of cut to correlate the chip serration frequency with the prominent mode frequency of the machine tool components following the procedure described earlier.

Next the FFT output in power spectrum for Ti6Al4V alloy are analyzed and the highest vibration peaks and the corresponding excited frequencies at two different depth of cut are recorded. Typical FFT output in power spectrum at various cutting speed for these two depths of cut are shown in Fig. 14. From the different FFT outputs, it is observed that at 2.2 mm depth of cut, the maximum acceleration amplitude is observed at cutting speed of 30 m/min, whereas at 2.0 mm depth of cut, maximum acceleration amplitude is observed at the cutting speed of 40 m/min.

The primary serration frequency is again found to be more prominent at these two depths of cut. The primary serration frequencies for every cutting condition are calculated for these two depths of cut and are plotted against the cutting speed in Fig. 15. The chip serration frequency, which increases with cutting speed, is found to be lower for the lower depth of cut (2 mm), which may be due to the lower cutting temperature compared with that at the higher depth of cut (2.2 mm).

The acceleration amplitudes are plotted against the cutting speed for the two depths of cut in Fig. 16. From this figure, it can be observed that no severe vibrations are observed in the spindle's natural frequency range until the cutting speeds of 20 m/min for depth of cut 2.2 mm and 30 m/min for depth of cut 2.0 mm.

It can be further observed from Figs. 14–16 that when the chip serration frequency (3982 Hz) is approximately equal to the first natural frequency of the inner spindle (4394 Hz) at 30 m/min for the 2.2 mm depth of cut (Fig. 16), acceleration amplitude assumes the highest value (Figs. 14 and 16). It can be also observed for the 2.0 mm depth of cut that when the chip serration frequency (4088 Hz) is approximately equal to the same natural frequency at 40 m/min (Fig. 14), acceleration amplitude assumes the highest value

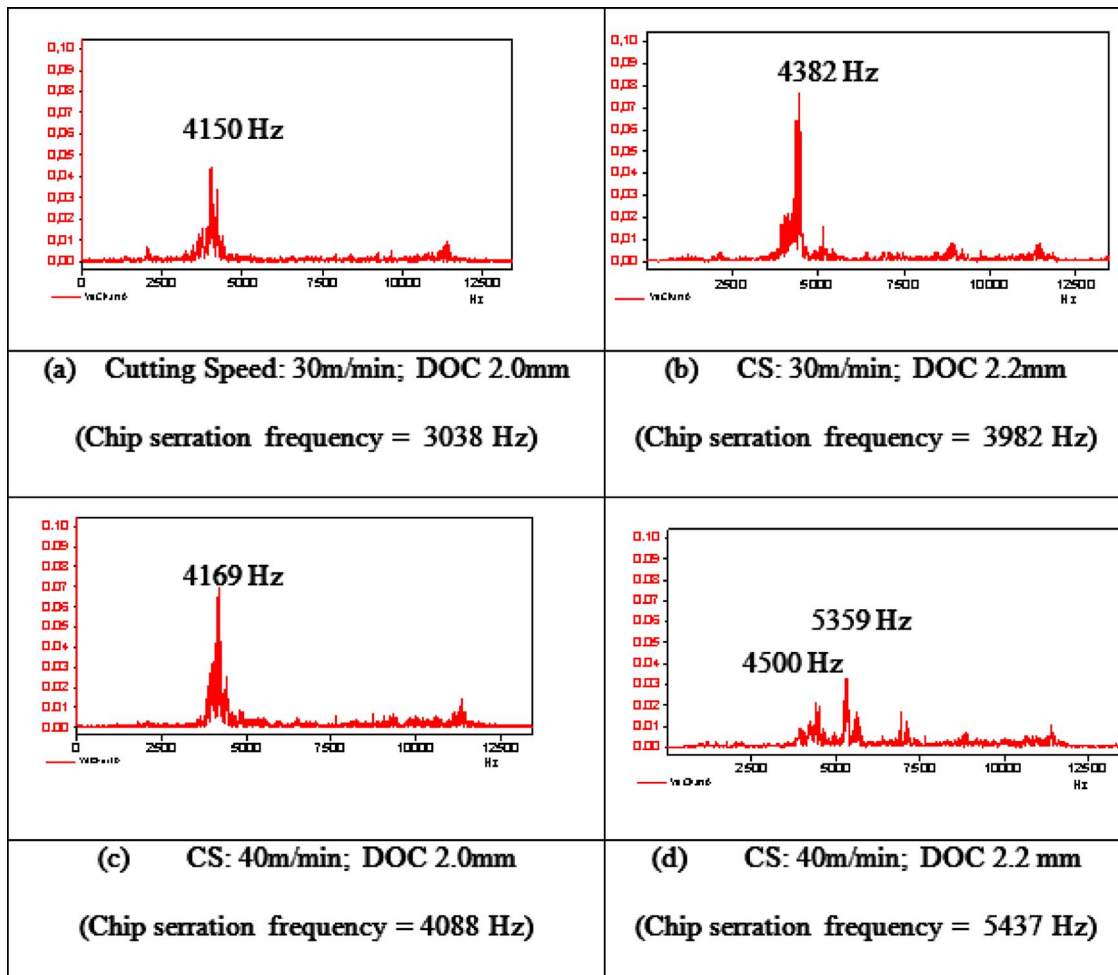


Fig. 14 FFT power spectra during machining for end milling at two different cutting speeds for two different depths of cut (2.0 mm and 2.2 mm)

(Figs. 14 and 16). For a depth of cut 2.2 mm, chatter is observed in the cutting speed range 20–40 m/min, whereas for a depth of cut 2.0 mm, the chatter is observed in the range 30–50 m/min because of the shift in the chip serration frequency and consequently a shift in cutting speed at which these frequencies coincide with the natural frequency of the spindle. It is finally observed that when the primary chip serration frequency shifts away from the prominent mode frequency zones, the cutting become more stable.

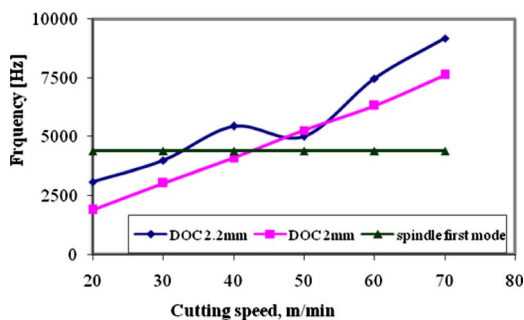


Fig. 15 Effect of depth of cut and spindle's natural frequency on chip serration and chatter frequency

3.5 Chip Morphology During End Milling of Ti6Al4V Alloy at Different Feeds. The different chips formed during end milling performed for different feed variations are collected and investigated to find out the primary and the secondary serrated teeth. It has been observed that with the variation of feed, the formation of primary serration is more prominent than that of the secondary serration.

The SEM views of the chips at different feed values are shown in Fig. 17. It has been observed that at low feed value, the primary serration frequency is very much higher than that of the high feed

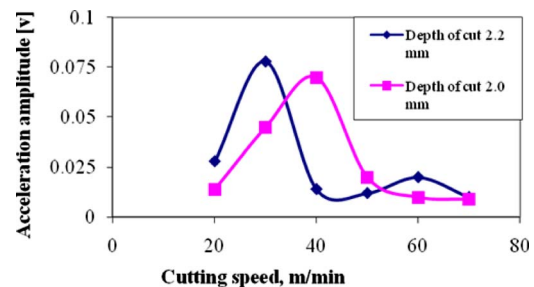


Fig. 16 Effect of depth of cut on acceleration amplitude

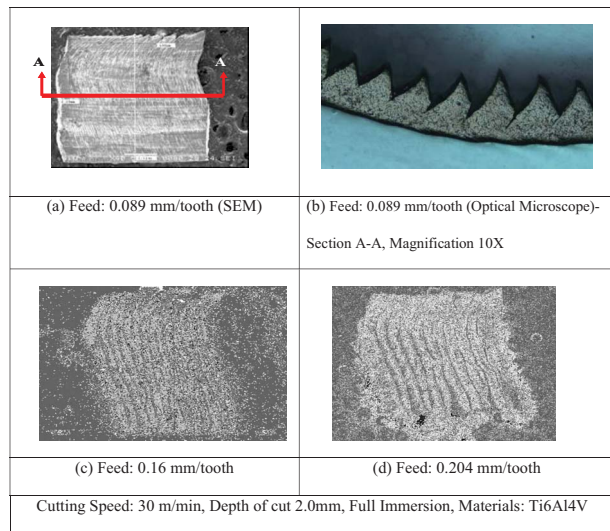


Fig. 17 Chip morphology—SEM view at different feeds

values, as shown in Fig. 17. The chip at low feed value needs to be further investigated to identify the primary serrated teeth because it is very difficult to measure the number of primary serrated teeth considering the SEM view of the chip. The low feed value chips are collected and chip specimens are prepared. The prepared chip specimens are polished and etched for viewing the optical microscope to capture the primary serration, as shown in Fig. 17(c).

3.5.1 FFT Analysis at Different Feeds. The online vibration monitoring data acquisition is used to capture the vibration data at different feed values for observation of chatter formation. The FFT outputs in power spectrum for machining of Ti6Al4V alloy are analyzed and the highest vibration peaks and the corresponding excited frequencies at every cutting condition are recorded. Typical FFT output in power spectrum at various cutting speeds for different depths of cut are shown in Fig. 18. From the FFT diagram, it has been observed that with the variation of feed, the chatter amplitude also varies. Chatter is observed at high feed values compared with low feed. At low feed, the primary serration is much higher than that of at high feed, as shown in Fig. 19; as a result, chatter is absent because high chip serration frequency do not coincide with the prominent mode frequencies. But at high feed, the chip serration is lower so chatter observed. It has also been found that chatter formation zone may also vary with the variation of cutting speed.

3.5.2 Effect of Different Feeds and Its Relationship Between Chip Frequency and Chatter Frequency. It is very important to identify the prominent serration frequency either primary or secondary from the chip morphology as discussed above. It has been observed that the primary serration frequency is more prominent for Ti6Al4V alloy at different feed values. The primary serration frequency for every feed values at different cutting speeds is calculated and frequency of saw teeth formation versus cutting speed for different feed values is shown in Fig. 19. It has been observed that for both the feed the chip serration, frequency is proportional to cutting speed. At different feed values, the chatter formation zones also vary because of the variation of the chip serration frequency. It has been found that at feeds 0.16 mm/tooth and 0.204 mm/tooth, the maximum acceleration amplitude is recorded at the cutting speed of 40 m/min because of the resonance effect of chip serration frequency with the first mode frequency of inner

spindle. But at low feed with the same cutting conditions, no severe vibration are observed because the primary chip serration frequency at low feed is very high compared with high feed.

Acceleration amplitude versus cutting speed is also plotted in Fig. 20 for two different feed values. In the spindle's natural frequency range, no severe vibrations are observed until the cutting speed of 30 m/min for both feed values because the chip frequency is below this natural frequency range, but amplitude starts to increase and attains the maximum value at 40 m/min for both the feed values because of the resonance effect between the primary chip serration frequency with the spindle first mode frequency, as shown in Fig. 20.

Acceleration amplitude is slightly higher in high feed values because the higher chip serration values (4178 Hz), which is almost the same with the first mode frequency of the inner spindle (4394 Hz).

From the above observations, it may be concluded that in the case of end milling, acceleration amplitudes are amplified and ultimately chatter appears in the system when the chip serration frequency is close to the spindle's natural frequency mode shape. The spindle may be termed as the "main weak" component in terms of chatter in end milling, since most severe vibrations of the spindle system starts when the chip frequency approaches the spindle's natural frequency mode shape. It may be finally concluded that the primary cause of chatter during machining is the instability of the chip formation process. Chatter appears in the system when the frequency of chip formation instability, associated either with the element chip or the secondary serrated teeth or the primary saw tooth formation, is close to the prominent natural frequency (or frequencies) of the system.

4 Conclusions

The following conclusions have been drawn from the work:

1. Investigations, involving observations of the top and sectional views of chips using SEM and optical microscope, respectively, show that the chips produced during end milling of Ti6Al4V exhibit regularly spaced serrated teeth along the main section of the chip in the entire cutting speed range. These teeth are formed due to the adiabatic nature of the shear process. The frequency of these serrated teeth increases with cutting speed and are also dependent on feed, depth of cut, and the system parameters.
2. On the other hand, the machine tool-work-piece-fixture system has various modes (natural frequencies), some of which play prominent role in chatter formation. It has been found that the natural frequencies of the inner and the outer spindles and the chuck play prominent role in chatter formation during end milling since high amplitudes of vibration occur when these components start vibrating at their natural frequencies with high amplitude.
3. Vibrations at the natural frequencies are excited when the chip serration frequency gets close to the corresponding natural frequencies upon variation of cutting speed, feed, or depth of cut. As a result, the chatter formation zone also varies with the variation of these cutting parameters, as well as the natural frequencies of the system.
4. Hence it may be concluded from these observations that chatter appears in the system during end milling of Ti6Al4V when the primary chip serration frequency gets close to one of the dominating mode shapes (natural frequencies) of the machine tool system (spindle in this particular case) as a result to resonance.

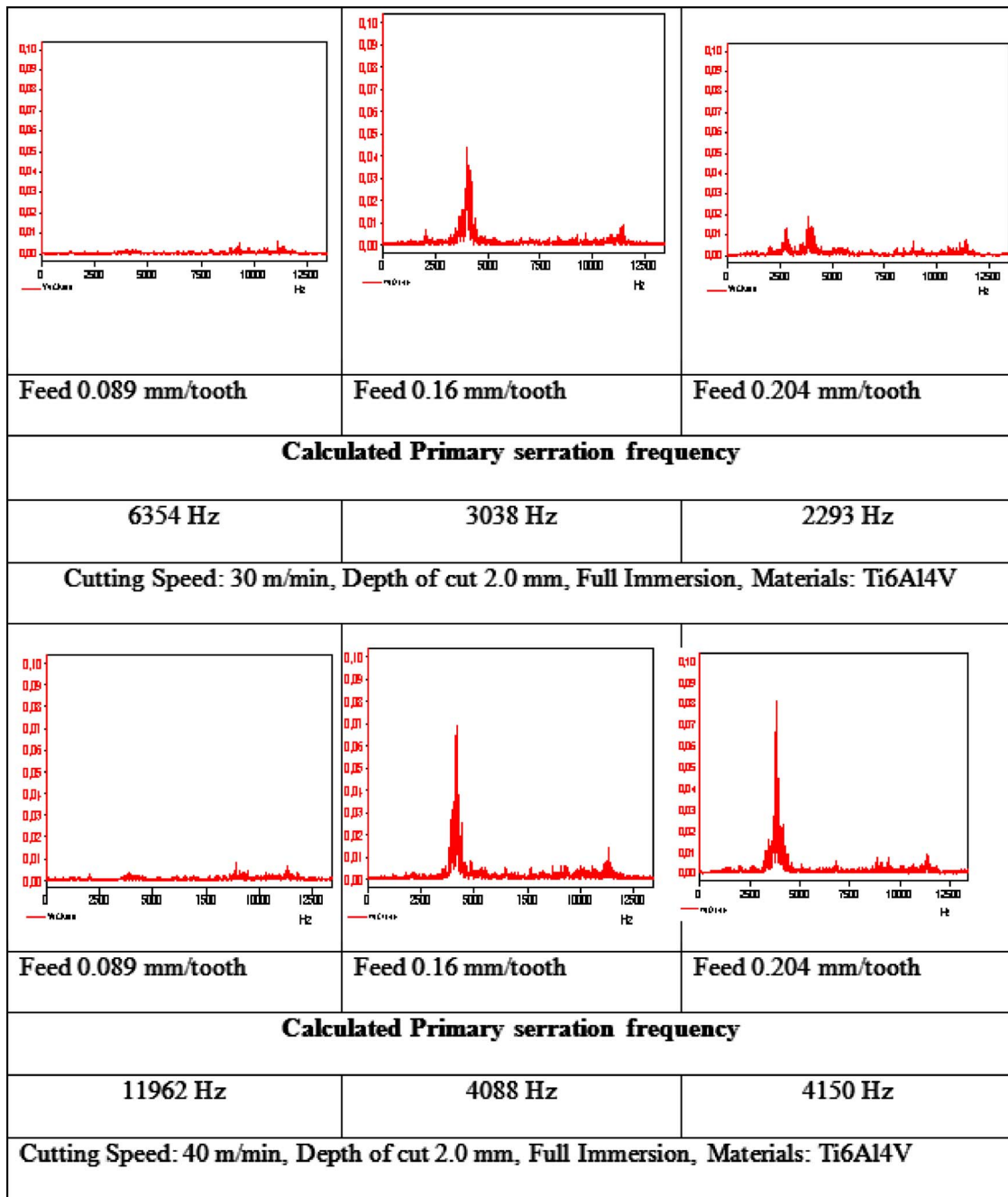


Fig. 18 FFT power spectrum during machining for end milling at two different cutting speeds with three different feed values

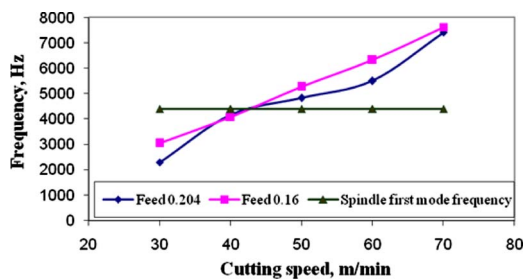


Fig. 19 Effect of feed on chip serration frequency and chatter formation

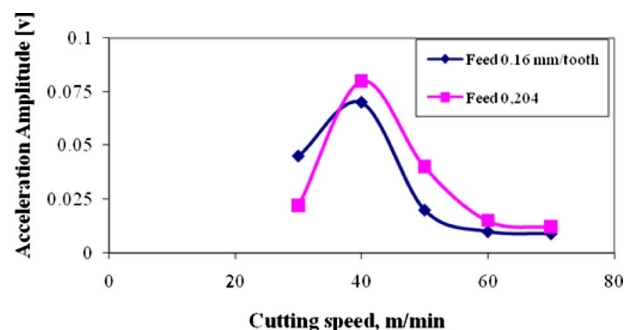


Fig. 20 Effect of feed on acceleration amplitude

References

- [1] Taylor, F. W., 1907, "On the Art of Cutting Metals," *Trans. Amer. Soc. Mech. Eng.*, **28**, pp. 31–350.
- [2] Kuznetsov, V. D., 1977, *Fizika Rezanja e Trenja Metallov e Kristalov*, Nauka, Moscow, p. 310.
- [3] Shteinberg, I. C., 1976, *Removal of Chatter Appearing During the Metal Cutting Process on Lathe Machine*, Machine Building, Moscow, in Russian.
- [4] Kudinov, V. A., 1965, *Dynamics of Machine Tools*, Machine Building, Moscow, in Russian.
- [5] Eliasberg, M. E., 1962, "Fundamentals of the Theory of Chatter During Metal Cutting Process," *Stanki i Instrumenti*, No. 10, pp. 3–8.
- [6] Loladze, T. H., 1980, *Chip Formation During Metal Cutting Process*, Machine Building, Moscow.
- [7] Doi, S., 1953, "On the Chatter Vibrations of Lathe Tools," *Memoirs of the Department of Mechanical Engineering, Nagoya University*, Vol. 5, p. 179.
- [8] Doi, S., and Kato, S., 1953, "Chatter Vibrations of Lathe Tools," *Trans. Amer. Soc. Mech. Eng.*, **78**, pp. 1127–1134.
- [9] Kato, S., 1958, "Theoretical Research on Chatter Vibration of Lathe Tools," *Memoirs of the Department of Mechanical Engineering, Nagoya University*, p. 117.
- [10] Smith, J. D., 1962, "The Dynamic Cutting of Metals," Ph.D. thesis, University of Cambridge, Cambridge, UK.
- [11] Smith, J. D., and Tobias, S. A., 1961, "The Dynamic Cutting of Metals," *Int. J. Mach. Tool Des. Res.*, **1**, pp. 283–292.
- [12] Tashlickii, N. I., 1960, *Primary Source of Energy Inducing Self-Oscillations When Cutting Metal*, *Vestnik Mashinostroeniija*, Moscow, in Russian.
- [13] Tobias, S. A., 1965, *Machine Tool Vibration*, Wiley, New York.
- [14] Amin, A. K. M. N., 1982, "Investigation of the Laws Governing the Formation of Chatter During Metal Cutting Processes and Their Influence on Tool Wear," Ph.D. thesis, Georgian Polytechnic Institute, Tbilisi, GA.
- [15] Patwari, A. U., Amin, A. K. M. N., Faris, W. F., and Ishtiyag, M. H., 2010, "Investigation of Formation of Chatter in a Non-Wavy Surface During Thread Cutting and Turning Operations," *Journal of Advanced Materials Research*, **83–86**, pp. 637–645.
- [16] Patwari, A. U., Amin, A. K. M. N., Faris, W. F., and Alam, S., 2008, "Investigations of the Causes of Chatter in Computer Aided Manufacturing Process During End Milling Operation," *Proceedings of the Third International Conference on Mechatronics 2008*, Faculty of Engineering, International Islamic University of Malaysia, Dec. 18–20, pp. 416–421.
- [17] Patwari, A. U., Amin, A. K. M. N., and Faris, W. F., 2010, "Role of Chip Serration Frequency in Chatter Formation During End Milling Operation of Stainless Steel," *Journal of Advanced Materials Research (AMR)*, **97–101**, pp. 1989–1992.
- [18] Armarego, E. J. A., 1969, *The Machining of Metals*, Prentice-Hall, Englewood Cliffs, NJ.
- [19] El Mansori, M., 2009, "Machinability of Ferromagnetic Steels by Magnetically-Assisted Cutting Process," AMPT Paper No. 131.
- [20] Amin, A. K. M. N., Ismail, A. F., and Nor Khairushhima, M. K., 2006, "Role of Discrete Nature of Chip Formation and Natural Vibrations of Prominent System Components in Chatter Formation During Metal Cutting," *Proceedings of the International Conference on Advances on Materials and Processing Technologies—AMPT 2006*, Jul. 30–Aug. 3, Las Vegas, NV.
- [21] Patwari, A. U., Amin, A. K. M. N., and Faris, W. F., 2009, "Finite Element and Experimental Analysis of Dynamic Behavior of Vertical Machining Centre Components by Modal Analysis," *Proceedings of International Conference of Advance Materials for Application in Acoustics and Vibration*, Jan. 4–6, Cairo, Egypt.
- [22] Komanduri, R., Schroeder, T., Hazra, J., von Turkovich, B. F., and Flom, D. G., 1982, "On the Catastrophic Shear Instability in High-Speed Machining of an AISI 4340 Steel," *Trans. ASME, J. Eng. Ind.*, **104**, pp. 121–131.
- [23] Patwari, A. U., Amin, A. K. M. N., and Faris, W. F., 2010, "A Coupled Artificial Neural Network and RSM Model for the Prediction of Chip Formation Instabilities in End Milling of Inconel 718," *International Conference on Computer and Communication Engineering (ICCCCE 2010)*, International Islamic University of Malaysia, Kuala Lumpur, Malaysia, May 11–12.
- [24] Patwari, A. U., Amin, A. K. M. N., and Faris, W. F., 2010, "Identification of Instabilities of Chip Formation and It's Prediction Model During End Milling of Medium Carbon Steel (S45C)," *American Journal of Engineering and Applied Sciences*, **3**(1), pp. 193–200.
- [25] Talantov, N. V., Amin, A. K. M. N., and Chereomushnikov, N. P., 1980, "Temperature Deformation Laws of Chatter Formation During Metal Cutting Process," *Abstracts of the Papers Presented at the Fifth Soviet National Conference Teplofizika Technologichieskikh Processov*.
- [26] Amin, A. K. M. N., Nashron, F. R., and Zubaire, W. W. D., 2006, "Role of the Frequency of Secondary Serrated Teeth in Chatter Formation During Turning of Carbon Steel AISI 1040 and Stainless Steel," *International Conference on Manufacturing and Materials Processing—ICMM 2006*, Kuala Lumpur, Malaysia, Mar. 14–15, pp. 246–251.
- [27] Amin, A. K. M. N., Hakim, I., and Venkatesh, V. C., 2004, "Investigations of the Primary Causes of Chatter During End Milling on Vertical Machining Centre (VMC)," *Proceedings of the International Conference ICAMT 2004*, pp. 179–186.